Conductivities and Spectroscopic Studies of Polymer Electrolytes Based on Linear Polyurethane and Hybrid and Copolymer of Linear and Hyperbranched Polyurethanes

Ling Hong,*,† Liyi Shi,† and Xiaozhen Tang‡

Department of Chemistry, School of Science, Shanghai University, Shanghai 200436, China, and School of Chemistry and Chemical Technology, Shanghai Jiao Tong University, Shanghai 200240, China

Received February 26, 2003

ABSTRACT: Three polyurethane electrolytes, linear polyurethane (LPU), hybrid of linear and hyperbranched polyurethane (MHPU), and low cross-linked copolymer of linear and hyperbranched polyurethane (CHPU) complex with $LiClO_4$, were studied using conductivity, FTIR, Raman, and ^{13}C, ^{1}H, and ^{7}Li solid-state NMR measurements. The best conductivity value measured at 25 °C was 2.7×10^{-7} S cm^{-1} at about a EO/Li ratio of 8 for the LPU electrolytes. At a higher salt concentration (EO/Li = 4), the MHPU and CHPU electrolytes reached its maximum conductivity, 1.35×10^{-6} and 1.51×10^{-5} S cm^{-1}, respectively. FTIR, Raman, and ^{13}C NMR analysis showed that hyperbranched polymer could function as a "solvent" for the lithium salt. Correlation times and the activation energies for the polymer segmental and the lithium hopping motions were determined from the temperature dependence of the spin−lattice relaxation of the polymer (^{1}H) and lithium (^{7}Li). The correlation time and activation energy for the lithium hopping motions in the CHPU electrolytes had a relatively low value. This indicated that lithium ion transport was easier in such a system.

1. Introduction

Solid polymer electrolytes (SPEs) formed by complexing a polymer with alkali metal salts have received considerable attention, especially because of their potential applications in solid-state batteries and electrochromic devices. The ionic conductivity of SPE is due to the motion of dissolved ionic species in a polymeric matrix. It is well established that the ionic mobility is promoted by segmental motion of the polymer host and that the conduction takes place in the amorphous phase of the SPE.

The deliberate introduction of branches into polymeric materials has become a topic of considerable interest and activity in the past few years.[1−5] Hawker et al.[6] introduced a concept of hyperbranched polymer electrolytes. An interesting feature of the hyperbranched poly(ethylene glycol) (PEG) derivatives is their lack of crystallinity. Usually these hyperbranched show no melting points in the thermal analytical traces. Therefore, the amorphous nature of the hyperbranched macromolecules allows these materials to be successfully used as polymer electrolytes with no detrimental effects due to crystallization. The nonentangled state of hyperbranched macromolecules imposes rather poor mechanical properties and results in brittle polymer. This disadvantage could be avoided by copolymerized or mixed with linear polymer.

Infrared (IR) and Raman spectroscopy have proved to be powerful tools to probe salt−polymer interactions and the type of charge carriers responsible for the conduction by providing information in band positions, intensities, and band shapes. This is important for determining the species of the microstructures in the electrolyte by exploring the spectral changes of most of the interesting functional groups in the polymer electrolyte.

Most methods used to characterize the polymer electrolytes such as ionic conductivity, thermal properties, and others do not separate the roles of the anions and cations. Solid-state NMR has the advantage of being able to selectively measure the dynamics of the different species in the polymer electrolytes.[7−12] Measurements of spin−lattice relaxation rates as a function of temperature have been used to study the correlation between the cationic and the polymer chain segmental motions in SPEs.

In the present work, linear polyurethane, hybrid of linear and hyperbranched polyurethane, and low cross-linked copolymer of linear and hyperbranched polyurethane were selected separately as polymer matrix. Conductivity, the complex interaction behavior between polymer and $LiClO_4$ salt, and ^{1}H and ^{7}Li NMR spin−lattice relaxation measurements as a function of temperature in the polymer electrolytes were reported. The mobility of ions in SPE depends on the local dynamics of the polymer chain segments. Combined application of ^{1}H and ^{7}Li NMR measurements can give us real insight into the physical properties concerning both dynamics. By using FTIR, Raman, DSC, and solid-state NMR analysis, the effect of hyperbranched structure on conductivity of polymer electrolyte was investigated.

2. Experimental Section

Materials. $LiClO_4$ was dried under reduced pressure prior to use. The linear polyurethane (LPU) was synthesized from 4,4′-diphenylmethane diisocyanate (MDI), 1,4-butanediol (BD), and PEO (M_n = 1000). The molar ratio of MDI:BD:PEO was 3:2:1. The structural formula is as follows:

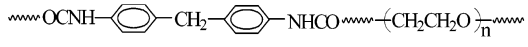

LPU

† Shanghai University.
‡ Shanghai Jiao Tong University.
* Corresponding author: Tel 86-21-56773440; e-mail HongL99@263.net.

10.1021/ma034243y CCC: $25.00
Published on Web 06/03/2003

The synthesis procedure of the hyperbranched polyurethane (HPU) has been described in detail in our previous report.[13] The structural formula is as follows:

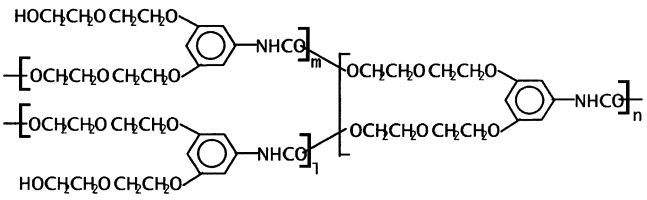

HPU

The hybrid of linear and hyperbranched polyurethane (MHPU) contained 30% of HPU.

Low cross-linked copolymer of linear and hyperbranched polyurethane (CHPU) was synthesis using the synthesis procedure of HPU. Part of BD was replaced by HPU, which had many hydroxyl groups in the terminal. Low cross-linked copolymer was acquired by controlling the ratio of NCO/OH. The weight percent of hyperbranched polyurethane in copolymer was also 30%.

Preparation of Polymer Electrolyte Film. The polymer and $LiClO_4$ were solvated in THF, and then the solution was cast into a Teflon plate. A film formed at ambient temperature, and it was dried in a vacuum oven at 60 °C for 48 h.

Conductivity Measurement. The complex impedance spectra were measured from 25 to 100 °C using a Hewlett-Packard 4192A LF impedance analyzer over a frequency range of 1 Hz−1 MHz. The films were cut to a required size (10 mm in diameter and 0.2−0.3 mm thick) and were sandwiched between two copper electrodes.

FTIR and Raman Measurement. The IR spectra were recorded at ambient temperature on a Perkin-Elmer model 963 FTIR spectrophotometer in the range 400−4000 cm^{-1} with a wavenumber resolution of 2 cm^{-1}. The Raman spectra were performed at room temperature in the range 50−3500 cm^{-1} with a wavenumber resolution of 2 cm^{-1}. The spectra were recorded on a Bruker model EQUINOX-55 infrared−Raman spectrophotometer with a Raman module FRA 106 and a near-infrared YAG laser with wavelength 1064 nm. Band deconvolution of the Raman spectra was obtained by using a Gaussian−Lorentzian sum, and a constant baseline had been subtracted in the deconvolution figures in order to do the analysis. The maximum error associated with the fit was estimated to less than 5%.

Solid-State NMR Measurement. High-resolution solid-state ^{13}C NMR experiments were carried out on a Bruker DSX-300 spectrometer operating at resonance frequencies of 300.13 and 75.47 MHz for ^{1}H and ^{13}C, respectively. The ^{13}C CP/MAS spectra were measured with 4.1 μs, 90° pulse angle, 500 μs contact time, 5 s acquisition time, and with 1000 scans. All NMR spectra were taken at 298 K with broad-band decoupling, normal cross-polarization pulse sequence, and a magic angle spinning (MAS) of 5 kHz.

The T_1 measurements were performed using the inversion recovery (i.e., 180°−t−90°−Acq). The 90° pulse widths for ^{1}H and ^{7}Li were 2.5 and 8.6 μs, respectively. For the ^{7}Li NMR operating was used at 116.6 MHz.

3. Results and Discussion

Ionic Conductivity. Figure 1 showed the salt concentration dependence of the conductivity and the lithium salt concentration from a EO/Li ratio (EO is the number of ether oxygen of the polymer) of 2.0 to 32 for the polymer electrolytes based on LPU, MHPU, and CHPU. The conductivity maximum, 2.7×10^{-7} S cm^{-1} at 25 °C, of linear polyurethane-based polymer electrolyte appeared at about a EO/Li ratio of 8. The conductivity based on MHPU and CHPU keeps increasing over a much larger range of salt concentration. At about the EO/Li ratio of 4, the conductivity reaches its maximum,

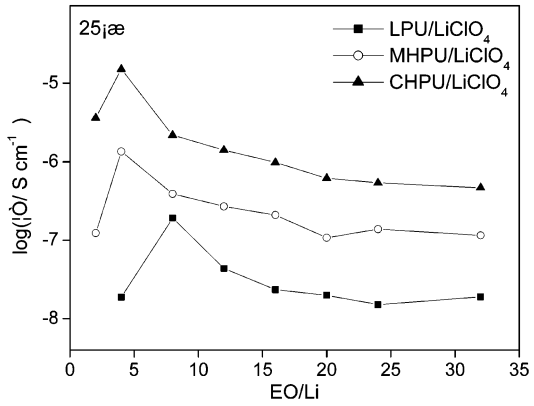

Figure 1. Salt concentration dependence of ionic conductivity of polymer electrolytes.

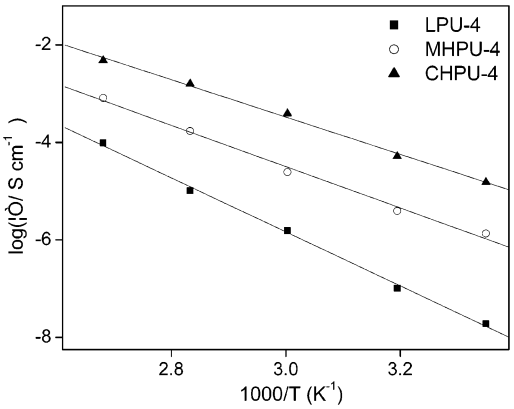

Figure 2. Temperature dependence of ionic conductivity of polymer electrolytes.

Table 1. Results of Regressing the Arrhenius Equation onto the Conductivity Data for the Polymer Electrolytes

sample	EO/Li	$\log(\sigma_0$/S $cm^{-1})$	E_A (kJ/mol)
LPU-4	4	10.74	46.05
MHPU-4	4	8.21	35.21
CHPU-4	4	7.99	31.79

1.35×10^{-6} S cm^{-1} for MHPU/$LiClO_4$ samples and 1.51×10^{-5} S cm^{-1} CHPU/$LiClO_4$ samples. After the maximum value, the conductivity decreases quickly with the increasing lithium salt concentration for all the three polymer electrolyte samples. This behavior is similar to most of the salt concentration dependences of polymer electrolytes.

At a EO/Li ratio of 4, the temperature dependence of the conductivity is shown in Figure 2. It could be found that the CHPU-4 sample had the highest conductivity. The difference in conductivity, measured for the three samples, can be interpreted as due to the different salt solvating capability, polymer chain segmental motions, and lithium hopping motions in the electrolytes.

The conductivity increased with increasing temperature. The temperature dependence of σ was well described by the Arrhenius equation

$$\sigma = \sigma_0 \exp[-E_a/RT] \qquad (1)$$

where σ_0 was preexponential factors and E_a was the activation energies. The parameter estimates determined from regressing eq 1 onto the data are given in Table 1.

FTIR Spectra Analysis. Polymer electrolytes based on LPU, MHPU, and CHPU show similar thermal and

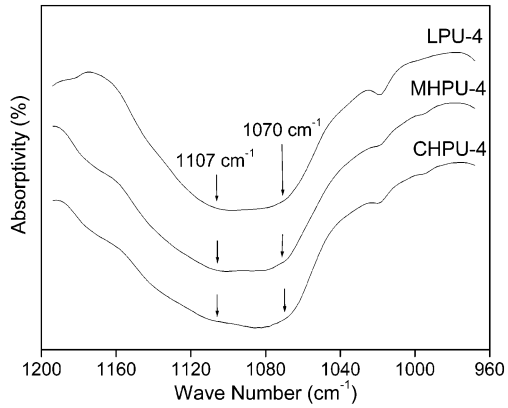

Figure 3. FTIR spectrum of LPU-4, MHPU-4, and CHPU-4 samples (ether group).

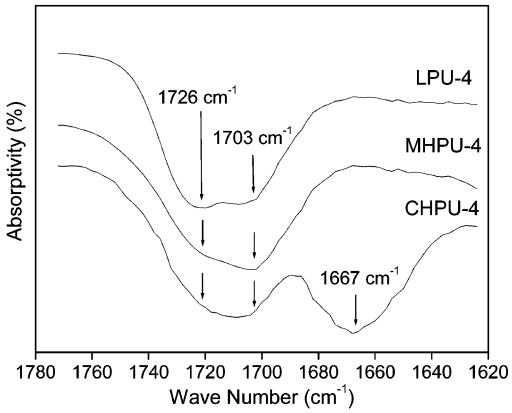

Figure 4. FTIR spectrum of LPU-4, MHPU-4, and CHPU-4 samples (carbonyl).

electrochemical behavior but exhibit different conduction performance. FTIR spectroscopy was employed to study the interaction behavior between the ion and the polymer host. Figure 3 showed the ether group absorption peaks of the LPU-4, MHPU-4, and CHPU-4 samples. The band centered at around 1107 cm^{-1} was attributed to the stretching of free ether groups, whereas the band at about 1070 cm^{-1} was assigned to the bonding degree of Li^+ with ether groups.[14] It could be found that the absorption of the bonded ether groups of MHPU-4 increased slightly more than that of LPU-4, and the absorption of the bonded ether groups of CHPU-4 increased slightly more than that of MHPU-4 corresponding to the free ether groups.

Figure 4 showed the carbonyl absorption peaks of the LPU-4, MHPU-4, and CHPU-4 samples. The band centered at about 1726 cm^{-1} was attributed to the stretching of free urethane carbonyl groups, whereas the band at about 1703 cm^{-1} was assigned to the bonding degree of Li^+ with carbonyl groups.[14−16] The absorption of the bonded carbonyl groups of MHPU-4 and CHPU-4 samples had a large increase than that of LPU-4 sample corresponding to the free groups. This indicated that the bonding degree of Li^+ in MHPU-4 and CHPU-4 samples was higher than that in LPU-4 sample, and the addition of hyperbranched polymer was helpful to improve the coordination degree of carbonyl groups with Li^+.

It was interesting to find that a third band centered at about 1667 cm^{-1} appeared in the curve of CHPU-4 sample. According to our research, this band was not observed at low salt concentration (EO/Li ≥30). This band could be attributed to bonded carbonyl groups and might be related to the characteristics of carbonyl groups in low cross-linked copolymer of linear and hyperbranched polyurethane. It was obviously that this low cross-linked structure further improved the coordination degree of carbonyl groups with lithium ion.

It has been commonly accepted that lithium interacts to a certain extent with the oxygen in the oxyethylene segment in a polymer electrolyte. In the conduction process, the lithium ion moves from one oxygen coordination site to another. From the FTIR analysis, it could be found that carbonyl also play an important role in the conduction process in polyurethane electrolyte systems.

Raman Spectra Analysis. The Raman spectra band between 920 and 960 cm^{-1} was associated with the anion symmetric stretching mode (ν_1). It is usual to investigate this band to study the ion−ion interaction. Figure 5 showed the three Lorentzian fittings of the ν_1 band. The first peak (peak I) around 931 cm^{-1} was very close to the frequency of the ν_1 band of perchlorate anion in solution, which was assigned to free ions.[17−20] The second peak (peak II) around 938 cm^{-1} was usually assigned to ion pairs.[19,21] The third peak (peak III) around 945 cm^{-1} observed in the spectra indicated the presence of trimers, tetramers, or higher order ionic clusters of sub-microscale (aggregates).[17,21] The fourth Lorentzian peak around 957 cm^{-1} was not observed here, which frequency corresponds to that of the salt crystal.[19,20]

The fraction of ion pairs and aggregates of MHPU-4 was lower than that of LPU-4. When copolymerization and low cross-link occurred in CHPU-4, the salt aggregates disappeared and the area fraction of ion pairs also decreased to 9.4% (Table 2). Combined with the result of FTIR analysis, it could be concluded that the hyperbranched polymer could dissolve more salt and function as a "solvent" for the lithium salt, and the copolymerization between hyperbranched and linear polyurethane enhanced this function.

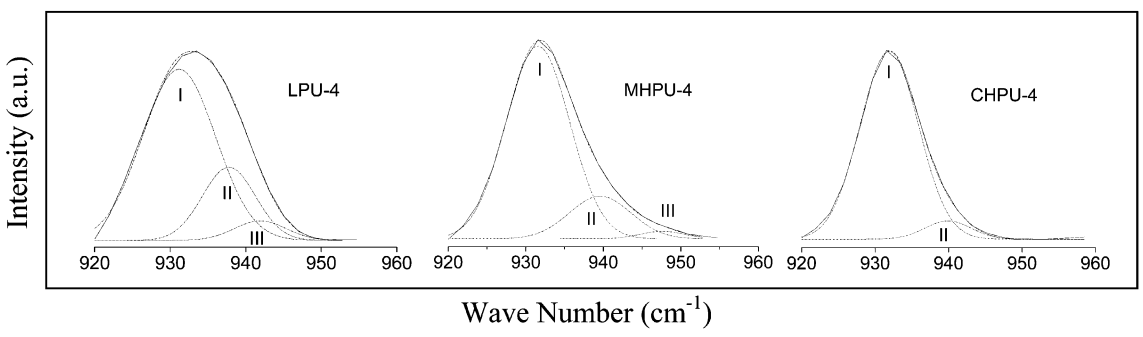

Figure 5. Raman band associated with the ClO_4^- ν_1 mode fitted by the sum of Lorentzian lines.

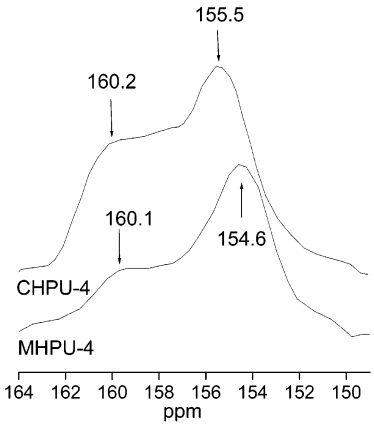

Figure 6. ^{13}C CP/MAS NMR spectra of C═O peaks at room temperature.

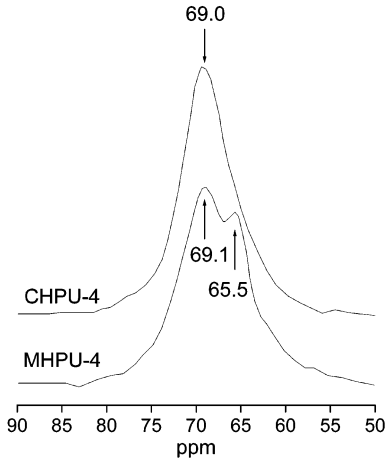

Figure 7. ^{13}C CP/MAS NMR spectra of CH_2CH_2O peaks at room temperature.

Table 2. Relative Proportions of the Different Ionic Species for the Polymer Electrolytes

		peak area (%)		
sample	EO/Li	I	II	III
LPU-4	4	70.2	24.7	5.1
MHPU-4	4	81.5	17.1	1.4
CHPU-4	4	90.6	9.4	0

Solid-State NMR Analysis. The ^{13}C CP/MAS NMR spectrum was used to characterize the interaction behavior between polyurethane and $LiClO_4$ complex. Figures 6 and 7 showed the scale expanded ^{13}C CP/MAS NMR spectra of C═O and CH_2CH_2O peaks of MHPU-4 and CHPU-4 at room temperature. The C═O resonance of the polyurethane was assigned at 150−162 ppm, which has two peaks: one centered at about 155 ppm and the other centered at about 160 ppm. This means two different states of carbonyl existed. The areas of peak at about 160 ppm of CHPU-4 increased compared to that of MHPU-4. The peak at 50−85 ppm was assigned to the resonance of the CH_2CH_2O group in polyurethane electrolytes. The resonance of the MHPU-4 had two peaks: one centered at about 69.0 ppm and the other centered at about 65.5 ppm, which could not be found in the curve of CHPU-4. This indicated a different coordination degree between urethane carbonyl, ether group, and lithium ion in the MHPU-4 and CHPU-4 samples.

Figure 8 shows the temperature dependence of ^1H and ^7Li spin−lattice relaxation time. The magnetization recovery toward equilibrium in these systems is found to be an exponential described by a single T_1 value. T_1 minima were observed in each of the samples for ^1H and ^7Li resonances.

The spin−lattice relaxation time at the Larmor frequency ω_0 peaks at a given temperature, T_{min}, at which the condition $\omega_0\tau_c = 2\pi\nu_0\tau_c \approx 1$ is fulfilled. For the ^1H and ^7Li resonances, $\nu_0 = 300.13$ and 116.6 MHz, respectively. We could get a value for the correlation time, τ_c, for the motion causing the relaxation. In most cases, assuming a thermally activated process, the relaxation time will depend on temperature through an effective correlation time expressed by an Arrhenius function.

$$\tau_c = \tau_0 \exp[E_A/RT] \tag{2}$$

The Bloembergen, Purcell, and Pound (BPP) equation described homonuclear spin−lattice relation by dipole−dipole interaction[22]

$$\frac{1}{T_1} = C\left(\frac{\tau_c}{1+\omega_0^2\tau_c^2} + \frac{\tau_c}{1+4\omega_0^2\tau_c^2}\right) \tag{3}$$

where

$$C = \frac{3}{10}\gamma^4\hbar^2\sum_j \frac{1}{r_j^6} \tag{4}$$

γ is the gyromagnetic, r is the separation between dipoles (e.g., the H−H distance), and the summation index j is over all interacting dipoles.

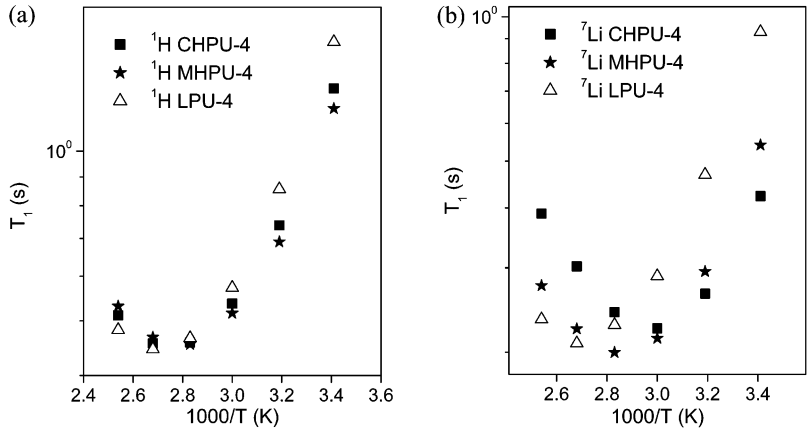

Figure 8. Temperature dependence of the ^1H and ^7Li spin−lattice relation time (T_1).

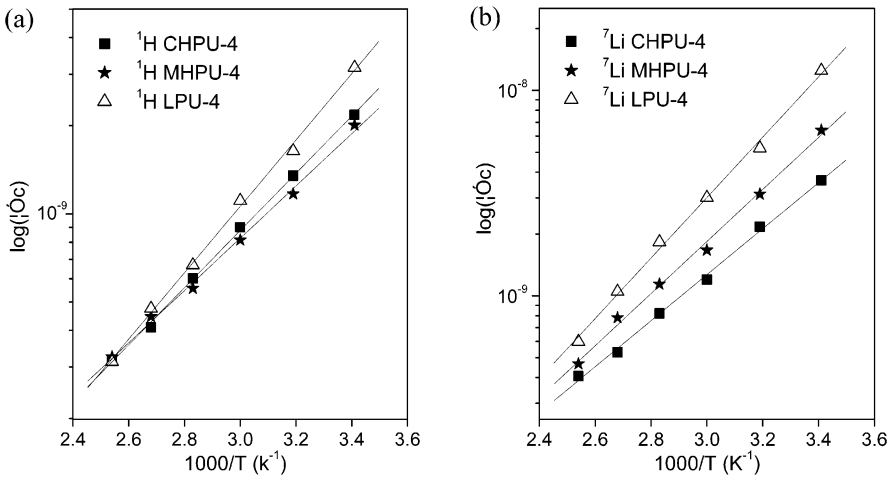

Figure 9. Temperature dependence of the ^{1}H and ^{7}Li correlation time (τ_c).

Table 3. E_A and τ_0 Obtained from the Spin−Lattice Relaxation Times

	polymer segmental motion		lithium hopping motion	
sample	$\tau_0 \times 10^{12}$ (s)	E_A (kJ/mol)	$\tau_0 \times 10^{12}$ (s)	E_A (kJ/mol)
LPU-4	0.36	21.6	0.13	27.8
MHPU-4	2.05	17.0	0.14	24.3
CHPU-4	1.00	18.5	0.58	21.2

In a similar way, the T_1 of the lithium resonance ^{7}Li ($I = {}^3/_2$) due to the quadrupolar mechanism can be analyzed by eq 3 by redefining C as

$$C = \frac{\omega_q^2}{50} \tag{5}$$

where ω_q is the hyperfine quadrupolar coupling constant.

Using eqs 2 and 3, it was possible to calculate τ_c at every temperature as shown in Figure 9. The E_A and preexponential factors, τ_0, of the polymer segmental and ^{7}Li hopping motions determined from the τ_c values were tabulated in Table 3.

The polymer undergoes the fast segmental motions and correlated hopping motions of the lithium ions located in the polymer chain occur in the time scale of 10^{-10}−10^{-8} s depending on the temperature. The motional parameters derived from relaxation data suggest that the segmental and lithium ion motion are affected by the different structure of polymer. The LPU sample has the highest correlation time τ_c and the activation energy E_A. This may be attributed to the crystallization of oligio(ethylene glycol) segment in linear polyurethane which restrict the mobility of polymer segment. When hyperbranched polyurethane was added to the host in MHPU-4, the amorphous nature of the hyperbranched macromolecules entered into the domain of soft segment in linear polyurethane and destroyed the ordered structure. The segmental motion and the lithium ion motion in MHPU electrolytes were easier, which could be characterized from the lower τ_c and E_A.

The correlation time and the activation energy of segmental motion in CHPU-4 increased slightly more than that in MHPU-4 due to the low cross-link occurring between the linear and hyperbranched polymer. However, the low cross-link structure between the linear and hyperbranched polymer ameliorated the nonentangled state of hyperbranched macromolecules and promoted the mobility of lithium ions between the hyperbranched macromolecules. So the lithium ion motion of CHPU-4 was the easiest in the three samples.

4. Conclusion

Polymer electrolytes based on LPU, MHPU, and CHPU doping with $LiClO_4$ were studied. FTIR, Raman, and ^{13}C NMR analysis showed that the hyperbranched polymer improved the coordination degree between lithium ion and polymer and was helpful to prevent the formation of ion pair and aggregates. This indicated that hyperbranched polymer could function as a "solvent" for the lithium salt and provide more ionic particles participating in conduction. The copolymerization between hyperbranched and linear polyurethane in CHPU enhanced this function. This performance was consistent with the result of conductivity. The conductivity CHPU/$LiClO_4$ samples reached its maximum, 1.51×10^{-5} S cm^{-1}, at a higher salt concentration about the EO/Li ratio of 4.

^{1}H and ^{7}Li NMR spin−lattice relaxation measurements as a function of temperature in the polymer electrolytes were reported. The mobility of ions in SPE depends on the local dynamics of the polymer chain segments. The addition of hyperbranched polymer improved the mobility of polymer chains and lithium ions and thus improved the conductivity. The low cross-link structure between the linear and hyperbranched polymer kept this excellent property and overcame the unfavorable influence of nonentangled state on ionic transmission. So this structure allowed these materials to be suitable used as polymer electrolytes

Acknowledgment. We gratefully acknowledge the financial support of the National Nature Science Foundation of China.

References and Notes

(1) Peerling, H. W. I.; Van Benthem, R. A. T. M.; Meijer, E. W. *J. Polym. Sci., Part A: Polym. Chem.* **2001**, *39*, 3112−3120.

(2) Vetter, S.; Koch, S.; Schlu&die er, A. D. *J. Polym. Sci., Part A: Polym. Chem.* **2001**, *39*, 1940−1954.

(3) Desai, A.; Atkinson, N.; Rivera, F. J.; Devonport, W.; Rees, I.; Branz, S. E.; Hawker, C. J. *J. Polym. Sci., Part A: Polym Chem.* **2000**, *38*, 1033−1044.

(4) Ashootosh, V.; Ambade, Kumar, A. *J. Polym. Sci., Part A: Polym. Chem.* **2001**, *39*, 1295−1304.

(5) Voit, B. *J. Polym. Sci., Part A: Polym. Chem.* **2000**, *38*, 2505−2525.
(6) Hawker, C. J.; Chu, F.; Pomery, P. J.; Hill, D. J. T. *Macromolecules* **1996**, *29*, 3831−3838.
(7) Forsyth, M.; Smith, M. E.; Meakin, P.; Macfarlane, D. R. *J. Polym. Sci., Part B: Polym. Phys.* **1994**, *32*, 2077−2084.
(8) Vincent, C. A. *Electrochim. Acta* **1995**, *40*, 2035−2040.
(9) Jahansson, A.; Gogoll, A.; Tegenfeldt, J. *Polymer* **1996**, *8*, 1387−1393.
(10) Roux, C.; Gorecki, W.; Sanchez, J. Y.; Belorizky, E. *Electrochim. Acta* **1998**, *43*, 1575−1579.
(11) Asano, A.; Takegoshi, K.; Hikichi, K. *Polym. J.* **1999**, *31*, 602−608.
(12) Tambelli, C. E.; Donoso, J. P.; Regiani, A. M.; Pawlicka, A.; Gandini, A.; LeNest, J. F. *Electrochim. Acta* **2001**, *46*, 1665−1672.
(13) Hong, L.; Cui, Y. J.; Wang, X. L.; Tang, X. Z. *J. Polym. Sci., Part A: Polym. Chem.* **2002**, *40*, 344−350.
(14) Fery, A.; Jacobsson, P. *Polymer* **1996**, *37*, 737−744.
(15) Zhu, W. H.; Wang, X. L.; Yang, B.; Tang, X. Z. *J. Polym. Sci., Part B: Polym. Phys.* **2001**, *39*, 1246−1254.
(16) Wen, T. C.; Luo, S. S.; Yang, C. H. *Polymer* **2000**, *41*, 6755−6764.
(17) Silva, R. A.; Silva, G. G.; Pimenta, M. A. *Electrochim. Acta* **2001**, *46*, 1687−1694.
(18) Stevens, J. R.; Jacobsson, P. *Can. J. Chem.* **1991**, *69*, 1980−1984.
(19) James, D. W.; Mayes, R. E. *Aust. J. Chem.* **1982**, *35*, 1775−1784.
(20) James, D. W.; Mayes, R. E. *Aust. J. Chem.* **1982**, *35*, 1785−1792.
(21) Cazzanelli, E.; Musrarelli, P.; Benevelli, F.; Appetecchi, G. B.; Croce, F. *Solid State Ionics* **1996**, *86*−*88*, 379−384.
(22) Bloembergen, N.; Purcell, E. M.; Pound, R. V. *Phys. Rev.* **1948**, *73*, 679−712.

MA034243Y